Detection of Optic Neuritis on Routine Brain MRI without and with the Assistance of an Image Postprocessing Algorithm

A. Schroeder, G. Van Stavern, H.L.P. Orlowski, L. Stunkel, M.S. Parsons, L. Rhea, and A. Sharma

ABSTRACT

BACKGROUND AND PURPOSE: At times, there is a clinical need for using routine brain MR imaging performed close to the time of onset of patients' visual symptoms to firmly establish the diagnosis of optic neuritis. Our aim was to assess the diagnostic performance of radiologists in detecting optic neuritis on routine brain MR images and whether this performance could be enhanced using a postprocessing algorithm.

MATERIALS AND METHODS: In this retrospective case-control study of 60 patients (37 women, 23 men; mean age, 47.2 [SD, 17.9] years), 2 blinded neuroradiologists evaluated T2-weighted FLAIR and contrast-enhanced T1WI from brain MR imaging for the presence of imaging evidence of optic neuritis. Images were processed using an image-processing algorithm that aimed to selectively accentuate the signal intensity of diseased optic nerves. We assessed the effect of image processing on the contrast-to-noise ratio between the optic nerves and normal-appearing white matter and on the diagnostic performance of the neuroradiologists, including the interobserver reliability.

RESULTS: The average sensitivity of readers was 55%, 56.5%, and 30.0% on FLAIR, coronal contrast-enhanced T1WI, and axial contrast-enhanced T1WI, respectively. Sensitivities were lower in the absence of fat saturation on FLAIR ($P = .001$) and coronal contrast-enhanced T1WI ($P = .04$). Processing increased the contrast-to-noise ratio of diseased (P value range $= .03$ to $<.001$) but not of control optic nerves. Processing did not improve the sensitivity but improved the specificity and positive predictive value. Interobserver agreement improved from slight to good.

CONCLUSIONS: Detection of optic neuritis on routine brain MR imaging is challenging. Specificity, positive predictive value, and interobserver agreement can be improved by postprocessing of MR images.

ABBREVIATIONS: CE = contrast-enhanced; CNR = contrast-to-noise ratio; ON = optic nerve; PPV = positive predictive value

Optic neuritis typically presents as a unilateral optic neuropathy characterized by decreased visual acuity, orbital pain exacerbated by extra-ocular movement, a relative afferent pupillary defect, and, occasionally, optic disc swelling.[1-8] Symptoms generally improve, and about 60% of patients regain full visual acuity within 2 months.[9] MR imaging, often used to confirm the diagnosis, is especially useful in atypical cases.[5] Dedicated MR imaging of the orbits obtained with and without intravenous

contrast has a reported sensitivity of 76.1%–100% when performed within 30 days of symptom onset.[10-13] This sensitivity decreases with time since the onset of vision loss, and the mean duration of optic nerve (ON) enhancement, even with triple-dose gadolinium administration, is only 63 days.[13]

While the clinical diagnosis of typical optic neuritis may be straightforward for neuro-ophthalmologists, misdiagnosis by other providers who often encounter the patients at the time of initial presentation reportedly occurs in up to 60% of referrals.[14] The combination of the self-limiting nature of the disease, frequent misdiagnosis at the initial encounter, long referral wait times, and decreased sensitivity of imaging in a delayed setting presents a diagnostic challenge: Neuro-ophthalmologists often have to rely on the imaging ordered by other providers to confirm the diagnosis. Often, this initial imaging is a routine brain MR imaging rather than a dedicated orbital MR imaging.

Most studies documenting the role of imaging in the detection of optic neuritis have focused on dedicated orbital MR imaging.

Table 1: Scan parameters for axial 2D FLAIR,[a] coronal CE-T1WI, and axial CE-T1WI used in the study

	FLAIR[a,b]	Coronal CE-T1WI[b]	Axial CE-T1WI[b]
Section thickness (mm)	5	5	5
TR (ms)	8000–11,000	300–742	276–780
TE (ms)	82–142	9–17	8.4–20
TI (ms)	2000–2500	–	–
FOV (mm)	172–230 × 210–230	172–230 × 172–230	172–230 × 210–230
Matrix	224–512 × 256–512	224–512 × 256–512	224–384 × 256–512
Subset of scans obtained with fat saturation	19 (63.3%)	17 (73.9%)	6 (20%)

Note:— – indicates N/A.
[a] In 3 patients, FLAIR images had been acquired using a 3D sequence with a 1-mm section thickness of images reconstructed in the coronal plane (TR = 5000 ms, TE = 395 ms, TI = 1800 ms, FOV = 256 × 256 mm, matrix = 256 × 256).
[b] For patients with optic neuritis, 19/30 (63.3%), 17/23 (73.9%), and 6/30 (20%) FLAIR, coronal CE-T1WI, and axial CE-T1WIs were performed using fat saturation.

The objective of this study was 2-fold. First, we aimed to assess the diagnostic performance of radiologists in detecting optic neuritis on routine brain MR imaging. Second, we sought to evaluate whether the diagnosis of optic neuritis on routine brain MR imaging could be facilitated using an image-postprocessing algorithm that has previously been shown to be helpful in the detection of optic neuritis on dedicated orbital MR imaging.[15] We hypothesized that the diagnostic accuracies of radiologists in detecting optic neuritis on routine brain MR imaging would be lower than the previously reported rates and that these could be improved by increasing the contrast-to-noise ratio (CNR) of the diseased ON by image postprocessing.

MATERIALS AND METHODS
The institutional review board at Washington University in Saint Louis approved this retrospective study and waived the need for consent for the use of pre-existing data.

Cases and Controls
This was a retrospective case-control study of 60 patients (37 women, 23 men; mean age 47.2 [SD, 17.9] years) who had undergone brain MR imaging, including T2-weighted FLAIR and CE-T1WI sequences. Patients were selected from the clinical database of 1 neuro-ophthalmologist and were seen during a 4-year period dating from June 2015 to June 2019. All patients with clinically proven unilateral optic neuritis were included if brain MR imaging performed within 4 weeks of symptom onset was available. The clinical diagnosis was established in all cases by an expert neuro-ophthalmologist based on clinical presentation, ophthalmologic examination, and evaluation of all relevant investigations. This search generated 30 patients with 30 eyes diagnosed with clinically proven optic neuritis. An equal number ($n = 30$) of brain MRIs of patients with third, fourth, or sixth cranial neuropathies but with clinically proven normal ON function were included as controls.

Images and Image Processing
For each patient, we included available FLAIR images to assess ON signal alteration and available CE-T1WI to assess ON enhancement. Imaging had been performed with variable scan parameters (Table 1). FLAIR, coronal CE, and axial CE images were available for 30 cases and 58 control eyes, for 23 cases and 44 control eyes, and for 30 cases and 58 control eyes, respectively.

FLAIR images were in the axial plane except in 3 patients in whom coronal reformations from the 3D-FLAIR sequence were used. Enhancement of the ONs was assessed individually on axial CE-T1WI, and, when available, on coronal CE-T1WI. Images were acquired using 1.5T (Magnetom Espree, Magnetom Aera, Magnetom Avanto, or Magnetom Sonata; Siemens) or 3T (Magnetom Trio or Magnetom Skyra; Siemens) scanners.

A blinded investigator processed these images using a proprietary algorithm (CIE; Correlative Enhancement) on a Horos workstation (https://horosproject.org/) using a custom-built plug-in. The processing involved the manual placement of an ROI to define the normal white matter signal. If the images were originally obtained with fat saturation, the algorithm accentuated the signal intensity of the ONs if the ON signal was determined to be significantly higher than this reference (Fig 1). For images that did not have inherent fat saturation, the algorithm was chosen to accentuate the signal intensity of the ON only if it fell in a range that was higher than the normal white matter intensity but lower than the intensity of fat (Fig 1F, -J, -L), while decreasing the intensity of fat (Fig 1F, -L). The processed images were saved as separate DICOM series for further analysis.

Blinded Imaging Review
Two blinded board-certified neuroradiologists rated each ON Horos FLAIR and CE images on a 5-point Likert scale, ranging from 1 (definitely normal) to 5 (definitely abnormal). For subsequent analyses, ratings of 4 (probably abnormal) or 5 were taken as abnormal test results, while ratings ≤3 (possibly normal) were taken as a normal test result. Reviewers first rated the ONs on baseline images; then, after a gap of several days, they again rated the ONs with the availability of both baseline and processed images.

Quantitative Analysis
We manually measured the signal intensities of each ON (SI^{on}) and the ipsilateral normal-appearing white matter (SI^{wm}) for both baseline and processed images on each sequence. For ONs with obvious signal abnormality, the ROI was placed in the region of abnormal signal. Otherwise, the ON was sampled in its retrobulbar portion on an image that allowed its best visualization, free from partial volume averaging effects. Using the SD of the signal intensity of air in the image as a measure of noise, we calculated the CNR for each sequence using the following formula: $CNR = (SI^{on} - SI^{wm})/Noise$.
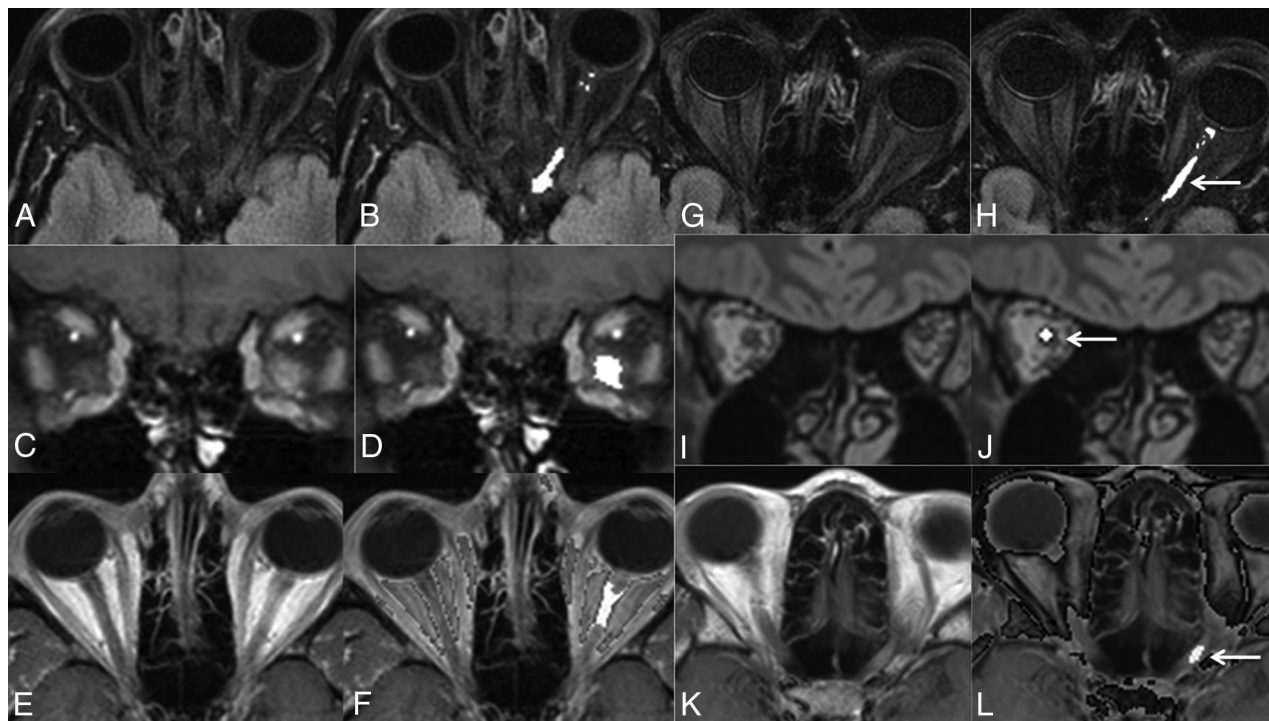
FIG 1. Axial FLAIR (*A* and *B*), coronal CE-T1WI (*C* and *D*), and axial CE-T1WI (*E* and *F*) images from routine brain MR imaging of a patient with clinically proven left optic neuritis before (*A, C,* and *E*) and after (*B, D,* and *F*) processing with a proprietary postprocessing algorithm showing accentuation of the signal intensity of the diseased optic nerve and the unaffected contralateral optic nerve. Axial FLAIR (*G* and *H*), coronal 3D-FLAIR (*I* and *J*), and axial CE-T1WI of different patients with clinically proven unilateral optic neuritis again demonstrating accentuation of intensity in diseased optic nerves (*arrows*) after processing (*H, J,* and *L*). Note that the detection of alteration in the optic nerve signal is especially challenging in images obtained without fat saturation (*E, I,* and *K*).

Statistical Analysis

Diagnostic performance for each reader and the average for both readers were assessed for baseline images in terms of sensitivity, specificity, positive predictive value (PPV), and negative predictive value for each sequence. Subset analysis was performed for images obtained with and without fat saturation. We quantitated the interrater reliability of confidence ratings for each sequence using κ (kappa).

Descriptive statistics were used to summarize the data. Continuous variables were summarized using means [SD] and medians (25th–75th percentiles), and categoric data were summarized using counts and percentages. The difference between cases and controls was tested using the nonparametric Kruskal-Wallis test for continuous variables and the Pearson χ^2 or Fisher exact test for categoric variables, as appropriate.

The effect of image processing on the confidence of categorization was assessed nonparametrically. The median of the scores across all readers and by individual readers, for cases and controls, was identified for both images, and the difference in the median (processed baseline image) was computed and compared using a signed rank test. Comparisons for each parameter pre- and postprocessing by an individual reader were performed using nonparametric signed rank tests.

Parameters for diagnostic performance and the interrater reliability of confidence ratings for reads with the availability of processed images were calculated and compared with corresponding parameters for baseline images to assess the effect of processing on readers' diagnostic performance. We used the McNemar test for paired and Fisher exact test for unpaired binary diagnostic accuracy statistics, including sensitivity, specificity, and diagnostic accuracy.

RESULTS

Diagnostic Performance of Radiologists in the Detection of Optic Neuritis on Brain MR Imaging without Postprocessing

On FLAIR, sensitivities for readers 1 and 2 were 57% and 53% (Table 2), lower for images without fat saturation (*P* = .001, Table 3). Corresponding specificities were 62% and 90%, respectively (Table 2).

On coronal CE-T1WI, readers 1 and 2 identified abnormal enhancement in 48% and 57% of cases with specificities of 82% and 95%, respectively (Table 2). Detection of contrast-enhancement was negatively impacted by the absence of fat saturation (*P* =.04). Sensitivities were much lower on axial CE images but not significantly decreased in the absence of fat saturation (*P* = .4, Tables 2 and 3).

Quantitative Analysis of Images before and after Processing

For images before processing, there was a significant difference between the CNR of the diseased and control ONs for FLAIR (*P* < .001) and coronal CE-T1WI (*P* < .001), but not for axial CE-T1WI (*P* = .17, Table 4).

Table 2: Results of diagnostic performance of 2 neuroradiologists in the detection of changes of optic neuritis on T2-weighted FLAIR, coronal CE-T1WI, and axial CE-T1WI of brain without and with the availability of postprocessed images that aimed to selectively accentuate the signal intensity of diseased optic nerves

	Reader 1			Reader 2			Average	
Parameter	Before Processing	After Processing	P^a Value	Before Processing	After Processing	P^a Value	Before Processing	After Processing
Sensitivity (FL)	56.7%	56.7%	.34	53.3%	53.3%	.31	55.0%	55.0%
Specificity (FL)	62.1%	89.7%	.01	89.7%	93.1%	.5	75.9%	91.4%
Accuracy (FL)	59.3%	72.9%	.03	71.2%	72.9%	.5	65.3%	72.9%
PPV (FL)	60.7%	85%	NA	84.2%	88.9%	NA	72.5%	86.9%
NPV (FL)	58.1%	66.7%	NA	65%	65.9%	NA	61.5%	66.3%
Sensitivity (CCE)	47.8%	56.5%	.31	56.5%	56.5%	.24	52.2%	56.5%
Specificity (CCE)	81.8%	100%	.07	95.5%	100%	.5	88.7%	100%
Accuracy (CCE)	64.4%	77.8%	.04	75.5%	77.8%	.5	69.9%	77.8%
PPV (CCE)	73.3%	100%	NA	92.9%	100%	NA	83.1%	100%
NPV (CCE)	60%	68.8%	NA	67.7%	68.8%	NA	63.9%	68.8%
Sensitivity (ACE)	20.0%	30.0%	.22	13.3%	30.0%	.07	16.7%	30.0%
Specificity (ACE)	86.2%	100%	.07	100%	100%	0	93.1%	100.0%
Accuracy (ACE)	52.5%	64.4%	.04	55.9%	64.4%	.07	54.2%	64.4%
PPV (ACE)	60%	100%	NA	100%	100%	NA	80.0%	100%
NPV (ACE)	51%	58%	NA	52.7%	58%	NA	51.9%	58%

Note:—FL indicates FLAIR; CCE, coronal CE-T1WI; ACE, axial CE-T1WI; NPV, negative predictive value; NA, not applicable.
[a] One-tailed McNemar test.

Table 3: Effect of fat saturation on the sensitivity of readers in detecting changes of optic neuritis on FLAIR and CE images before and after postprocessing

	Reader 1		Reader 2	
Sequence Type	Fat Saturation+	Fat Saturation−	Fat Saturation+	Fat Saturation−
FL before processing	13/19 (68.4%)	4/11 (36.6%)	12/19 (63.1%)	4/11 (36.4%)
FL after processing	12/19 (63.2%)	5/11 (45.5%)	11/19 (57.9%)	5/11 (45.5%)
CCE before processing	10/17 (58.8%)	1/6 (16.7%)	11/17 (64.7%)	2/6 (33.3%)
CCE after processing	12/17 (70.6%)	1/6 (16.7%)	12/17 (70.6%)	1/6 (16.7%)
ACE before processing	1/6 (16.7%)	5/24 (20.8%)	2/6 (33.3%)	2/24 (8.3%)
ACE after processing	2/6 (33.3%)	7/24 (29.2%)	2/6 (33.3%)	7/24 (29.2%)

Note:—FL indicates FLAIR; CCE, coronal CE-T1WI; ACE, axial CE-T1WI.

Table 4: Effect of processing on the CNR of optic nerves relative to ipsilateral normal-appearing white matter in cases with optic neuritis and controls with normal optic nerve function

Sequence Type	Median CNR (25th–75th Percentiles) for Optic Nerves with Optic Neuritis	P Value	Median CNR (25th–75th Percentiles) for Normal Optic Nerves	P Value
FL before processing	−1.05 (−46.7−81.3)	<.001	−12.7 (−86.9−106.9)	.25
FL after processing	54.4 (−46.7−795.6)		−12.7 (−86.9−137.9)	
CCE before processing	9.8 (−181.8−129.2)	<.001	2.6 (−83.2−179.1)	.50
CCE after processing	6.2 (−181.8−238.1)		−0.37 (−83.2−66.8)	
ACE before processing	11.8 (−29.6−267.8)	.03	−14.3 (−63.1−2.5)	.27
ACE after processing	93.9 (−29.6−543.3)		−14.3 (−63.1−2.5)	

Note:—FL indicates FLAIR; CCE, coronal CE-T1WI; ACE, axial CE-T1WI.

The median (25th–75th percentiles) CNR of diseased ONs increased from −1.1 (−47−81) to 54 (−47−796) on FLAIR ($P < .001$), from 12 (−30−268) to 94 (−30−543) on axial CE-T1WI ($P = .03$), and from 10 (−182−129) to 6 (−182−238) on coronal CE-T1WI ($P < .001$) after processing. These group differences resulted from an increase in the CNR of 17/30 (57%), 8/30 (24%), and 14/23 (61%) cases on FLAIR, axial CE-T1WI, and coronal CE-T1WI, respectively.

The CNRs of control eyes as a group were not significantly affected by processing (Table 4). There were 2/58 false-positives on FLAIR image and none on CE images.

Effect of Processing on Confidence Ratings

For a subset of nerves with optic neuritis that showed accentuation of the CNR after processing, processing improved the confidence of both readers in categorizing nerves as abnormal. On average, an increase in rating was seen in 10.5/17 (62%), 3.5/13 (27%), and 7.5/9 (83%) cases on FLAIR, coronal CE, and axial CE images. The confidence rating never decreased in the presence of processing-related accentuation of the CNR. This favorable effect was associated with correct categorization of 3/17 (18%), 2/13 (15%), and 5.5/9 (61%) cases as abnormal, which were initially categorized as false-negatives. In cases in which imaging

remained unaffected after processing, there was a consistent decrease in the confidence rating of both readers with false-negative categorizations of 2.5/13 (19%), 1/10 (10%), and 1/16 (6.3%) FLAIR, coronal CE, and axial CE sequences, respectively, which were correctly categorized before processing. For all cases combined, the confidence ratings of readers were largely unaffected.

For control nerves, no change in the CNR was observed after processing in 55/58 (95%) FLAIR, 44/44 (100%) coronal CE, and 58/58 (100%) axial CE images. This lack of accentuation of the ON signal increased the confidence for both readers in categorizing ONs as normal. On average, an appropriate decrease in ratings was seen in 25/55 (45%), 20/44 (45%), and 32/58 (55%) controls on FLAIR, coronal CE, and axial CE images, respectively. There were no instances of an increase in rating in the absence of processing-related accentuation of the CNR. This favorable effect was associated with correct categorization of 5.5/58 (9.5%), 6/44 (14%), and 7.5/58 (13%) eyes as normal that were initially categorized as false-positives. In 3/58 (5%) controls with false-positive accentuation of the CNR, there was no increase in the false-positive rate because these eyes were categorized as false-positive even before processing. Overall, with image processing, there was a significant favorable shift in the median confidence ratings of controls for each reader on FLAIR ($P <.001$, .007), axial CE-T1WI ($P < .001$, .002), and coronal CE-T1WI ($P < .001$, .004) and a corresponding improvement in specificity (Table 2).

Effect of Processing on Diagnostic Performance

The sensitivities of readers were relatively unaffected (Table 2). There was an increase in the specificity of readers in detecting optic neuritis–related changes on all sequences, with the average specificity for the 2 readers increasing from 76% to 91% on FLAIR ($P = .01$ and .5 for the 2 readers), from 88.7% to 100% on coronal CE-T1WI ($P = .07$ and .5 for the 2 readers), and from 93% to 100% on axial CE-T1WI ($P = .07$ for reader 1, no change observed for reader 2) (Table 2). The overall diagnostic accuracy improved for one reader on FLAIR ($P = .03$ with either improvement or a trend towards improvement on other sequences (Table 2). Average PPVs for FLAIR, axial CE-T1WI, and coronal CE-T1WI improved from 73% to 87%, from 80% to 100%, and from 83% to 100%, respectively. Negative predictive values were relatively unchanged for other sequences. The overall trend was similar for subgroups with and without fat saturation (Table 3).

Interobserver agreement increased for all sequences after processing, with κ increasing from 0.08 to 0.67 on FLAIR, from 0.12 to 0.68 on axial CE-T1WI, and from 0.29 to 1 on coronal CE-T1WI.

DISCUSSION

In patients who happen to be evaluated by routine brain MR imaging at the time of symptom onset, there may still be a clinical need to evaluate this scan for imaging signs of optic neuritis. Our results indicate that in such scans that are not optimized for ON assessment, sensitivities for the detection of either signal alteration on FLAIR (55% in our study, Table 3) or abnormal contrast-enhancement (53% on coronal images, Table 3) are much lower

than the corresponding values of 76%–100% reported in the literature for dedicated orbital MR images.[10-13,15]

To the best of our knowledge, there is only 1 previous study investigating the diagnostic performance of brain MR imaging regarding the detection of optic neuritis on FLAIR images.[16] In this study, specifically on fat-suppressed FLAIR images, the authors reported a sensitivity of 76%–77%,[16] significantly higher than that in our study. This difference is likely because our study included images acquired from a multitude of scanners with inconsistent fat suppression. The detection of optic neuritis on MR imaging is assisted by fat-saturated sequences,[17] and our results support this finding (Table 3). Indeed, the sensitivity in our study was significantly affected by the presence or absence of fat suppression (Table 3), with an average sensitivity of 66% for a subgroup with fat-saturated FLAIR images being much closer to that reported previously by McKinney et al.[16]

No prior studies have explored the detection of ON enhancement in the setting of optic neuritis on routine brain CE sequences. With an average sensitivity of 53%, it is notable that in 74% of patients in our study (Table 1), coronal CE-T1WI had been performed with fat saturation. This is not always the case for routine brain MR imaging. For patients scanned without such a sequence, the sensitivity for the detection of ON enhancement can be substantially lower, with an average of 25% in our study (Table 3).

Because a coronal CE-T1WI may not always be included in a routine brain MR imaging protocol, we also assessed the ability of radiologists to detect the presence of enhancement on axial CE-T1WI. The average sensitivity for detecting ON enhancement in the axial plane (17%) was substantially lower, likely resulting from a combination of partial volume averaging effects, which is more likely to impact a horizontally extending ON in the axial plane, and an infrequent use of fat saturation in axial CE images (Table 1).

These challenges in detecting optic neuritis on routine brain MR imaging are also highlighted by only slight interobserver agreement for FLAIR and coronal CE-T1WI and fair interobserver agreement on axial CE-T1WI.

It has been previously shown that the detection of optic neuritis on FLAIR and CE-T1WI can be improved using an image-postprocessing algorithm that can selectively accentuate the CNR between diseased ONs and the normal white matter.[15] We observed a similar beneficial effect of the algorithm on the CNR of diseased ONs on FLAIR as well as CE-T1WI (Table 4 and Fig 1). While this resulted in an improvement of diagnostic accuracy, unlike in the previous study, this improvement in the CNR did not translate into improvement in the sensitivity for the detection of signal alterations on FLAIR images (Table 2). The analysis of change in confidence ratings indicates that this issue was at least partly a result of decreased confidence in assigning disease status in the cases in which the processed images failed to accentuate the CNR. We did, however, observe some improvement in sensitivity for the detection of ON enhancement (Table 2).

As reported previously,[15] rates of false-positive accentuation of signal in control ONs (3.4% for FLAIR and 0% for CE images) were low in our study. This finding translated into an improvement in the specificity and PPVs for FLAIR and CE images

(Table 2). Also, as seen previously, the availability of processed images resulted in substantial improvement in the interobserver agreement to substantial or almost perfect levels.[15]

In addition to use in patients presenting with optic neuritis, this processing could find use in patients with MS. While the ON is not currently a cardinal location, it has been recommended as a potential addition to diagnose MS at its early stages.[18] Sartoretti et al[19] have previously shown that patients with MS may have subclinical episodes of optic neuritis. Given that routine surveillance brain MR imaging is currently recommended to monitor disease progression,[20] this algorithm may be useful to detect clinical and/or subclinical optic neuritis in such scans.

A few limitations should be noted. First, our study used only 2 expert neuroradiologists as blinded readers who read each sequence only once. Intraobserver reliability, therefore, could not be evaluated. It is possible that in instances in which image processing did not produce any change in the original images of cases or controls, differences in ratings of original and processed images by a given reader could at least partly be due to intraobserver variability. Consistency of change in reader responses in the absence of processing-induced image alteration, however, indicates that the improved specificity seen in our study is indeed a beneficial effect of the algorithm. Additionally, the use of this algorithm by radiologists who are not subspecialized in neuroradiology could not be evaluated, restricting the evaluation of the use of this algorithm in communities without subspecialized care. While our study did include scans from different scanners and with different parameters, we think that this feature makes it more representative of the reality of clinical practice, in which the patients may present to expert neuro-ophthalmology services already having been scanned at varying facilities.

CONCLUSIONS

Assessment of routine brain MR imaging without optimized sequences for the assessment of the ON has relatively poor sensitivity (approximately 55%), modest specificity, and only slight-to-fair interobserver agreement for the detection of optic neuritis–related changes on FLAIR and CE-T1WI. The sensitivity can be expected to be even lower if FLAIR and/or coronal CE-T1WI images are acquired without fat saturation. By selectively accentuating the CNR of diseased-but-not-normal ONs, our image-postprocessing algorithm can improve the diagnostic performance of readers with improved specificity and PPVs, accompanied by a substantial improvement in interobserver agreement. The image processing, however, was unable to bring the sensitivity to a level comparable with the reported values for dedicated orbital MR imaging, which should still be the criterion standard examination if ordered within the appropriate timeframe.

REFERENCES

1. **The clinical profile of optic neuritis: experience of the Optic Neuritis Treatment Trial—Optic Neuritis Study Group.** *Arch Ophthalmol* 1991;109:1673–78 Medline

2. Rizzo JF 3rd, Lessell S. **Optic neuritis and ischemic optic neuropathy: overlapping clinical profiles.** *Arch Ophthalmol* 1991;109:1668–72 CrossRef Medline

3. Bee YS, Lin MC, Wang CC, et al. **Optic neuritis: clinical analysis of 27 cases.** *Kaohsiung J Med Sci* 2003;19:105–12 CrossRef Medline

4. Balcer LJ. **Clinical practice: optic neuritis.** *N Engl J Med* 2006;354:1273–80 CrossRef Medline

5. Toosy AT, Mason DF, Miller DH. **Optic neuritis.** *Lancet Neurol* 2014;13:83–99 CrossRef Medline

6. Hoorbakht H, Bagherkashi F. **Optic neuritis, its differential diagnosis and management.** *Open Ophthalmol J* 2012;6:65–72 CrossRef Medline

7. Keltner JL, Johnson CA, Spurr JO, et al. **Baseline visual field profile of optic neuritis: the experience of the optic neuritis treatment trial–Optic Neuritis Study Group.** *Arch Ophthalmol* 1993;111:231–34 CrossRef Medline

8. Fang JP, Donahue SP, Lin RH. **Global visual field involvement in acute unilateral optic neuritis.** *Am J Ophthalmol* 1999;128:554–65 CrossRef Medline

9. Wilhelm H, Schabet M. **The diagnosis and treatment of optic neuritis.** *Dtsch Arztebl Int* 2015;112:616–25; quiz 626 CrossRef Medline

10. Rizzo JF 3rd, Andreoli CM, Rabinov JD. **Use of magnetic resonance imaging to differentiate optic neuritis and nonarteritic anterior ischemic optic neuropathy.** *Ophthalmology* 2002;109:1679–84 CrossRef Medline

11. Bursztyn L, De Lott LB, Petrou M, et al. **Sensitivity of orbital magnetic resonance imaging in acute demyelinating optic neuritis.** *Can J Ophthalmol* 2019;54:242–46 CrossRef Medline

12. Kupersmith MJ, Alban T, Zeiffer B, et al. **Contrast-enhanced MRI in acute optic neuritis: relationship to visual performance.** *Brain* 2002;125:812–22 CrossRef Medline

13. Hickman SJ, Toosy AT, Miszkiel KA, et al. **Visual recovery following acute optic neuritis: a clinical, electrophysiological and magnetic resonance imaging study.** *J Neurol* 2004;251:996–1005 CrossRef Medline

14. Stunkel L, Kung NH, Wilson B, et al. **Incidence and causes of overdiagnosis of optic neuritis.** *JAMA Ophthalmol* 2018;136:76–81 CrossRef Medline

15. Stunkel L, Sharma A, Parsons MS, et al. **Evaluating the utility of a postprocessing algorithm for MRI evaluation of optic neuritis.** *AJNR Am J Neuroradiol* 2019;40:1043–48 CrossRef Medline

16. McKinney AM, Lohman BD, Sarikaya B, et al. **Accuracy of routine fat-suppressed FLAIR and diffusion-weighted images in detecting clinically evident acute optic neuritis.** *Acta Radiol* 2013;54:455–61 CrossRef Medline

17. Guy J, Mao J, Bidgood WD Jr, et al. **Enhancement and demyelination of the intraorbital optic nerve: fat suppression magnetic resonance imaging.** *Ophthalmology* 1992;99:713–19 CrossRef Medline

18. Thompson AJ, Banwell BL, Barkhof F, et al. **Diagnosis of multiple sclerosis: 2017 revisions of the McDonald criteria.** *Lancet Neurol* 2018;17:162–73 CrossRef Medline

19. Sartoretti T, Sartoretti E, Rauch S, et al. **How common is signal-intensity increase in optic nerve segments on 3D double inversion recovery sequences in visually asymptomatic patients with multiple sclerosis?** *AJNR Am J Neuroradiol* 2017;38:1748–53 CrossRef Medline

20. Giorgio A, De Stefano N. **Effective utilization of MRI in the diagnosis and management of multiple sclerosis.** *Neurol Clin* 2018;36:27–34 CrossRef Medline